Retrievals of thin cloud optical depth from a multifilter rotating shadowband radiometer

Qilong Min
Atmospheric Sciences Research Center, State University of New York, Albany, New York, USA

Everette Joseph
Department of Physics and Astronomy, Howard University, Washington, DC, USA

Minzheng Duan
Atmospheric Sciences Research Center, State University of New York, Albany, New York, USA

Received 9 July 2003; revised 23 September 2003; accepted 10 October 2003; published 17 January 2004.

[1] A method is developed for accurate retrieval of thin cloud optical depth from measurements of a multifilter rotating shadowband radiometer (MFRSR). A key feature of this technique is correction of strong forward scattering of solar radiation into the instrument's field of view, which causes underestimation of retrieved cloud optical depth. To develop the correction method, measurements from the MFRSR under various atmospheric conditions are simulated by using a modified DISORT code that can accurately compute radiative intensity for strong forward scattering by thin clouds. These simulations are used to develop a polynomial fitting technique that corrects forward scattering into direct beam component. The correction is then applied to real MFRSR measurements. First, temporal and spectral variations in direct beam observations are used to discriminate between aerosol and thin cloud conditions. The true thin cloud optical depth, then, is inferred by removing background aerosol optical depth and by applying the polynomial fitting technique to correct the forward scattering contribution. An analysis of uncertainties associated with this method is also conducted and the results show that the retrievals are accurate to better than 5% or 0.05 when optical depth is less than 1. *INDEX TERMS:* 0305 Atmospheric Composition and Structure: Aerosols and particles (0345, 4801); 0320 Atmospheric Composition and Structure: Cloud physics and chemistry; 0360 Atmospheric Composition and Structure: Transmission and scattering of radiation; 0394 Atmospheric Composition and Structure: Instruments and techniques; *KEYWORDS:* cloud, aerosol, radiative transfer, remote sensing, radiometer

Citation: Min, Q., E. Joseph, and M. Duan (2004), Retrievals of thin cloud optical depth from a multifilter rotating shadowband radiometer, *J. Geophys. Res.*, *109*, D02201, doi:10.1029/2003JD003964.

1. Introduction

[2] Clouds play key roles in the atmospheric energy balance and in the hydrological cycle and hence in the earth's climate system. Factors that govern transmission, reflection and absorption of radiation in a cloudy atmosphere include cloud microphysical properties, optical thickness, single scattering albedo, and phase function, as well as cloud geometry and the surface albedo. Considerable research has been conducted to understand the role of clouds in climate change, but observational evidence of even the sense of cloud feedback is still lacking, particularly how the optical thickness of clouds respond to climate perturbation. In the absence of such evidence, large uncertainty remains of the sensitivity of the climate system to doubling of CO_2 [*Intergovernmental Panel on Climate Change* (*IPCC*), 2001]. More substantial evidence of cloud properties and their spatial and temporal variation is therefore crucial to further advancement in the understanding of global climate change.

[3] Various efforts have been made to derive cloud optical and microphysical properties from passive radiometric measurements. *King et al.* [1997, and references therein] provide a comprehensive review of efforts to derive cloud optical properties from space-borne sensors measuring emergent radiation at the top of the atmosphere. For surface-based sensors, several retrieval algorithms have been proposed to infer cloud optical depth and effective radius. These include narrow band spectral measurements and broadband measurements for overcast clouds [*Leontieva and Stamness*, 1996; *Min and Harrison*, 1996a; *Dong et al.*, 1997], and normalized difference cloud indexes for broken clouds [*Marshak et al.*, 2000; *Baker and Marshak*, 2001]. All the methods referred to above utilize diffuse radiation measurements to retrieve optical properties of relatively thick clouds by applying a complex radiative transfer model with various assumptions. This approach, however, is inef-

0148-0227/04/2003JD003964$09.00

fective for clouds that are optically thin and that produce inhomogeneous scattering in the atmosphere, such as boundary layer cumulus, cirrus, and cirrostratus. These clouds are among the most common clouds and therefore the retrieval methods cited above may in effect fail to accurately observe a measurable amount of the global cloud optical properties due to violations of retrieval assumptions in one way or another. It is widely known that the properties of optically thin clouds can be determined from measurements of transmission of the direct solar beam using Beer's law. The accuracy of cloud optical properties determined in this way is compromised by contamination of the direct transmission by light that is scattered into the sensors field of view. This phenomenon is dominant under thin cirrus conditions, particularly in the case of cirrus clouds where strong forward scattering by ice crystals occurs; a Sun photometer captures this forward scattered radiation within its field of view (FOV) in addition to the attenuated direct solar beam. The unwanted scattered radiance will result in an overestimation of the cloud transmission, and further result in an underestimation of the derived cloud optical depth. Several researchers [*Raschke and Cox*, 1983; *Shiobara and Asano*, 1994] have devised correction schemes that remove the scattered forward radiance for retrieval of cloud optical depth from finite FOV photometer measurements, and the present study adds to this body of work as described below.

[4] Hundreds of the multifilter rotating shadowband radiometers (MFRSR) have been deployed globally. The MFRSR is a seven-channel radiometer with six passbands 10 nm FWHM centered near 415, 500, 610, 665, 862, and 940 nm, and an unfiltered silicon pyranometer [*Harrison et al.*, 1994]. It uses an automated shadowbanding technique to measure the total-horizontal, diffuse-horizontal, and direct-normal spectral irradiances through a single optical path. It guarantees that the separated spectral irradiance components share the same passbands and calibration coefficients; hence the Langley regression of the direct-normal irradiance taken on clear stable days can be used to extrapolate the instrument's response to the top of the atmosphere, and this calibration can then be applied to both components of irradiance. Transmittances can be subsequently calculated under cloudy conditions as the ratio of the uncalibrated output to the extrapolated top-of-the-atmosphere value. *Min and Harrison* [1996a] have developed a family of inversion methods to infer optical properties of warm clouds from diffuse measurements of a MFRSR at 415 nm channel, using a nonlinear least squares method (NLSM) in conjunction with an adjoint formulation of radiative transfer [*Min and Harrison*, 1996b]. In this study, we take advantage of simultaneous spectral measurements of direct and diffuse transmittances of a MFRSR and temporal variations to retrieve optical depths for optically thin clouds from direct beam irradiance. A key feature of this work is that it develops a technique that corrects for contamination of the measured direct transmittance by strong forward scattering, and thereby considerably improves the accuracy of the retrieved properties. This paper is organized as follows: in section 2, we derive the retrieval method for aerosol and apparent thin cloud optical depth based on spectral and temporal characteristics of observed clouds and aerosols. Further, we estimate the true cloud optical depth by correcting the forward scattering contribution into the instrument's FOV. We accomplish this by developing a simple correction scheme that we derive from simulating MFRSR measurements of thin clouds using a fast radiation transfer model. This radiation transfer model is developed by combining the delta-fit method [*Hu et al.*, 2001] with synthesis of the singly- plus multiply-scattered intensities [*Nakajima and Tanaka*, 1988]. In section 3, we apply this retrieval algorithm to actual measurements obtained by an MFRSR that is deployed at the Atmosphere Radiation Measurement (ARM) Southern Great Plaint (SGP) site and investigate the consistency and uncertainty of the algorithm.

2. Retrieval Algorithm of Optically Thin Clouds

[5] For direct beam, the Bouguer-Lambert-Beer law can be written as

$$I^{dir} = \exp\left[-\left(\tau_{ray} + \tau_{gas} + \tau_{aer} + \tau_{cld}\right)A_0\right] \tag{1}$$

where I^{dir} is the transmittance of direct beam at the solar air mass A_0, which depends on the solar zenith angle. τ_{ray}, τ_{gas}, τ_{aer}, and τ_{cld} are optical depths of Rayleigh scattering, gaseous absorption, aerosol extinction, and cloud extinction, which are strongly wavelength dependent.

[6] The optical depth of Rayleigh scattering is approximated as [*Hansen and Travis*, 1974]

$$\tau_{ray} = 0.008569\lambda^{-4}\left(1 + 0.0113\lambda + 0.00013\lambda^2\right)P/P_0 \tag{2}$$

where the wavelength, λ, is in micrometers, and we use the average pressure, P, at the site relative to sea level pressure, P_0. The Rayleigh optical depth at the most sensitive channel (415) is uncertain to about 0.004 for variations of 10 mb from the standard pressure assignment and variations of temperature, humidity, and pressure profiles.

[7] The interference of gaseous absorption on retrievals is minimized by using the 415 and 860 nm channels for our retrieval. At these channels only ozone has a small impact on transmittance, and an assumption of ozone absorption at 300 Dobson Units results in ozone optical depths of 0.0001 and 0.0015 for 415 nm and 860 nm channels, respectively. The uncertainty of ozone optical depth due to variations of boundary layer ozone concentrations from the assumption of 300 Dobson Units is also negligible, less than 0.0002.

[8] In general, aerosol size distributions follow a power law agreement, which leads to the following Angstrom's empirical relationship between aerosol optical depth and wavelengths [*Angstrom*, 1929; *Junge*, 1963]:

$$\tau_{aer}(\lambda) = \beta\lambda^{-\alpha} \tag{3}$$

where β and α are constants determined as

$$\begin{aligned} \alpha &= -\ln\left(\tau_{aer}^{415}/\tau_{aer}^{860}\right)/\ln(0.415/0.860) \\ \beta &= \tau_{aer}^{415}/0.415^{-\alpha} \end{aligned} \tag{4}$$

[9] The Angstrom exponent α is an indicator of aerosol particle size because it ranges from 4 to 0 corresponding to

sizes that are valid for scattering in the Rayleigh and Mie scattering regimes, respectively. Observations show that continental aerosols have a typical value of 1.3 with a slight seasonal variation [*Michalsky et al.*, 2001]. The other constant, β, in the Angstrom relationship is related to the extent of aerosol loading in the atmosphere, which changes more rapidly than the size of aerosol particles. The fact that these two coefficients change on different temporal scales can be exploited as a means of characterizing aerosols in retrievals.

[10] Clouds, with particle sizes much larger than the wavelength of light, show extremely weak wavelength dependence; thus the following simple linear relationship is used to link optical depths at 415 and 860 nm

$$\tau_{cld}^{415} = \sigma \tau_{cld}^{860} \tag{5}$$

where the coefficient is about 0.989 and 0.968 for water and ice clouds, respectively [*Hu and Stamnes*, 1993; *Fu*, 1996].

[11] Under normal atmospheric conditions, Rayleigh and ozone optical depths are relatively fixed with only very minor variations. Therefore, we assume that Rayleigh and gaseous optical depths are constant and defined as given above. After removal of molecular scattering and absorption, the apparent optical depths (logarithm of measured direct beam) at 415 and 860 nm channels are

$$\begin{aligned} \tau^{415} &= \beta 0.415^{-\alpha} + \tau_{cld}^{415} \\ \tau^{860} &= \beta 0.860^{-\alpha} + \tau_{cld}^{415}/\sigma \end{aligned} \tag{6}$$

[12] There are three unknown parameters with two equations so to distinguish aerosol and cloud optical depths in the total apparent optical depth we rely on differences in the temporal and spectral characteristics of aerosols and clouds. When clouds are broken, which is usually the case for thin clouds, we can determine aerosol optical properties from direct beam measurements during the broken periods. For continental aerosols, the mean value of is about 1.3 with a minimum of 0.8 in the winter [*Michlasky et al.*, 2001]. Therefore, the following threshold values can be used to distinguish cloud and aerosol periods:

$$\alpha_{thre} = \begin{cases} 0.8 \max(\alpha); & a > 1 \\ 0.8; \text{ otherwise} \end{cases} \tag{7}$$

[13] This states that if the maximum value of α for a given day is greater than 1 then α_{thre} is set equal to 80% of that value otherwise it is set to 0.8. When the exponent α determined from both channels of 415 and 860 nm is larger than α_{thre}, we assume the period to be clear-sky. Otherwise we consider the period to be cloudy. Furthermore, the temporal scale of the presence of thin clouds over the sensor is on the order of minutes, while the temporal scale of aerosols is on the order of hours. Since the composition and size distribution of aerosols (which is related to the Angstrom's exponent α) change much slower than the number density of aerosols, we assume a constant value of α as α_{thre} during the presence of clouds. Both coefficients of β and τ_{cld}^{415} then are inferred from the 415 and 860 nm channels. The retrieved cloud optical depth (τ_{cld}^{415}) however, is considered to be an apparent optical depth because it is based on measurement of direct beam transmittance that includes light that has been scattered into the instruments FOV. Determining the true optical depth will require removal of this strong forward scattering contribution. This is addressed further in the following section.

3. Correction of Forward Scattering

[14] We develop a data set of simulated MFRSR measured intensities to correct for the forward scattering, but computing the radiation intensity of clouds is very challenging, particularly for the solar aureole region, because of the strong forward peak of the phase function. For the discrete ordinate methods, it requires a large number of the Legendre polynomial terms to represent the δ function-like forward peak feature. The δ-M method, which takes advantage of the fact that the higher-order terms in the Legendre polynomial expansion contribute primarily to the forward peak, truncates the Legendre polynomial to effectively remove the forward peak and has proven to be a most reliable means for flux computations [*Wiscombe*, 1977]. However, if there are insufficient streams in the expansion, the δ-M method results in oscillation of the truncated phase function and causes problems for radiance computations in both forward and backward directions. *Nakajima and Tanaka* [1988] proposed a procedure to yield the intensity field with an error of less than 1% by combining the δ-M method with exact computation of low orders of scattering. *Hu et al* [2000] developed a fast δ-fit method to accurately estimate the backscattered radiance by fitting the phase function with a small set of Legendre polynomial expansion coefficients. We modify the DISORT radiative transfer code [*Stamnes et al.*, 1988] by combining the δ-fit method with the Nakajima-Tanaka correction procedure to accurately and rapidly compute radiances in both forward and backward directions.

[15] In the DISORT, the total downward flux must be the same whether we use δ-fit scaling and forward scattering correction or not. That is,

$$F_d^-(\bar{\tau}) + \mu_0 F^S e^{-\bar{\tau}/\mu_0} = F_d^-(\tau) + \mu_0 F^S e^{-\tau/\mu_0} \tag{8}$$

where F^s, $F_d^-(\bar{\tau})$, and $F_d^-(\tau)$ are the Solar flux, the δ-fit scaled downward diffuse flux, and the unscaled downward diffuse flux, respectively. The optical depths with and without the δ-fit scaling are $\bar{\tau}$ and τ, respectively. The unscaled downward diffuse flux is recovered by

$$F_d^-(\tau) = F_d^-(\bar{\tau}) + \mu_0 F^S \left(e^{-\bar{\tau}/\mu_0} - e^{-\tau/\mu_0} \right)$$

[16] Further, the total downward diffuse intensity, I^T, is determined by combining the multiple scattering intensity based on the δ-fit scaling, I^M, and the low order scattering intensity based on the Nakajima-Tanaka procedure, I^L, as in

$$\begin{aligned} F_d^-(\tau) &= \int_0^{2\pi} d\phi \int_0^1 \mu I^T(\tau, \mu, \phi) d\mu = \int_0^{2\pi} d\phi \int_0^1 \mu \left(I^M + \varepsilon I^L \right) d\mu \\ &= F_d^-(\bar{\tau}) + \mu_0 F^S \left(e^{-\bar{\tau}/\mu_0} - e^{-\tau/\mu_0} \right) \end{aligned} \tag{9}$$

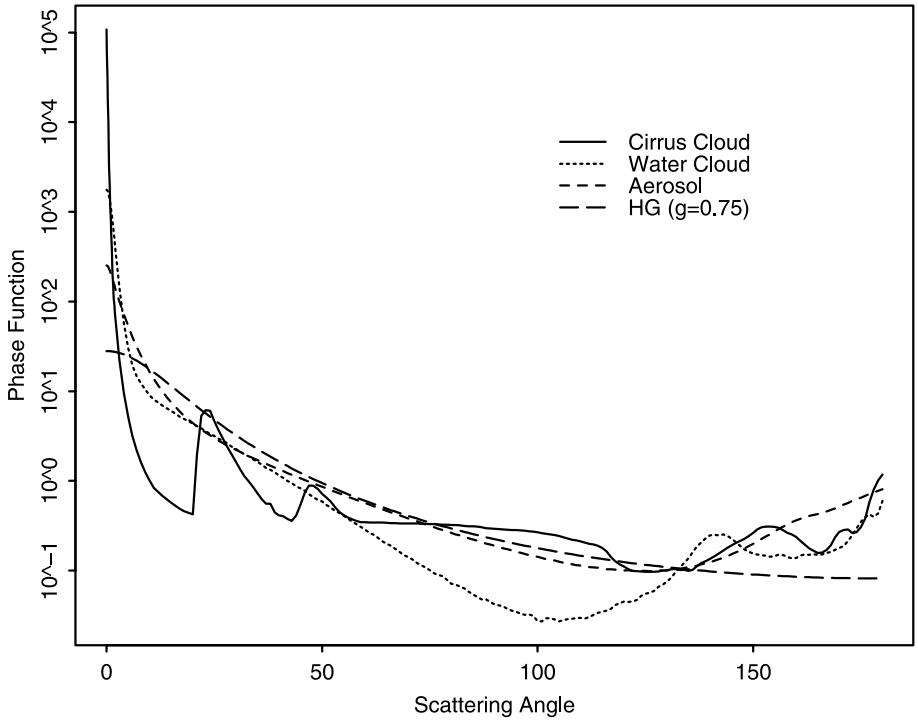

Figure 1. The phase functions of aerosol, water cloud, cirrus cloud, and HG with g = 0.75.

where the coefficient ε is adjusted to ensure consistency between the total downward diffuse intensity and the downward flux. Basically, we correct the intensity field according to accurate lower order scattering and simultaneously ensure consistency between the intensity and the flux.

[17] In the following simulations, we use the Air Force Geophysics Laboratory (AFGL) midlatitude model and aerosol profile from MODTRAN [*Berk et al.*, 1989]. We divide the atmosphere into 20 layers and confine the cloud layers at 1–2 km and 5–6 km for water and cirrus clouds, respectively. Figure 1 shows the phase functions used in our simulation, which for aerosols and water clouds are calculated using Mie theory. The phase function given by *Takano and Liou* [1989] for ice crystals is used for cirrus clouds. To get accurate radiance, we use 64 streams in the Legendre polynomial expansion. The simulated radiation intensities of water and cirrus clouds are shown in the Figure 2a and 2b, respectively. In both simulations, the cloud optical depth is 1 and the solar zenith angle is 45 degrees. Differences in the radiance field between the two cloud types are clearly evident in the Figure. Except for halos at 23 and 46 degrees for cirrus clouds, the solar aureole for cirrus clouds is much stronger and changes more rapidly than for water cloud.

[18] *Harrison et al* [1994] described the shadow band blocking mechanism and geometry of a MFRSR in detail. The shadow band blocks the sun with an umbral angle of 3.27 and polar angles from 0 to about 90 degrees. The MFRSR also takes measurements at 9 degrees on either sides of the solar-detector direction (two sided measurements) with the same block geometry to make a first order correction of the forward scattering contribution. Figure 3 shows the simulated direct beam measurements of the MFRSR at the 415 nm channel and its blocking components for a solar zenith angle at 45 degrees with slant-path optical depth from 0.412 to 5.6. The blocked diffuse component into the FOV of MFRSR (blocked_direct) increases with increasing optical depth and reaches a maximum at an optical depth of 2.0, and then decreases. The blocked diffuse components at both sides (blocked_side) increase with increasing optical depth. The difference of the blocked diffuse components between the sun direction and side directions is negligibly small for isotropic Rayleigh scattering and for small background aerosol conditions. The difference, however, increases significantly for increasing cirrus cloud optical depth when the optical depths are less than 2.0. For cloud optical depth 2.0 and greater the diffuse radiance becomes more isotropic and the difference of blocked diffuse components between both directions gradually reduces. Under cirrus cloud conditions, the first-order correction from side-blocking makes a small portion of the needed correction (10 to 25%), however, we would suggest that two more side-block measurements at smaller angles might improve the correction, particularly with a nonlinear correction scheme. The simulated direct transmittance of the MFRSR is substantially larger than the true direct transmittance. Therefore, without the correction of forward scattering, it will result in an underestimation of the cloud optical depth.

[19] Consideration of the observation geometry of the MFRSR indicates that the relationship between apparent optical depth (τ^P) and true optical depth (τ^T) is not linear and depends on the solar zenith angle. Therefore, for this relationship we propose the following polynomial fit

$$\tau^P = a/\mu_0 + b(\tau^T)^1 + c(\tau^T)^2 + d(\tau^T)^3 \qquad (10)$$

[20] In order to better account for the dependency of solar zenith angle, we fit our simulated observation for three

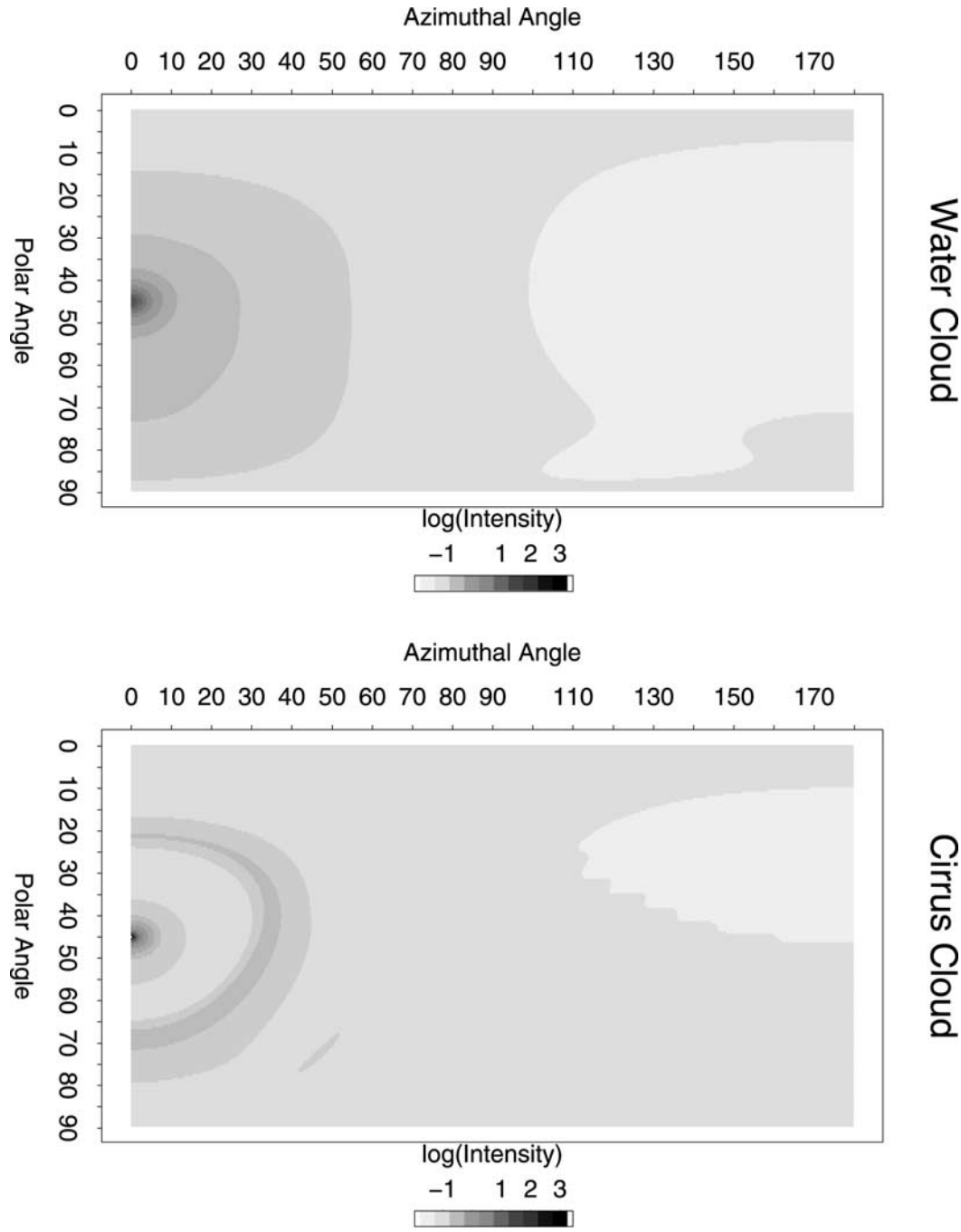

Figure 2. Simulated radiation intensities of water cloud and cirrus cloud.

intervals of solar zenith angle: less than 45, between 45 and 60, greater than 60 degrees. The fitting results for both water and cirrus clouds are listed in Table 1. It is difficult to distinguish between ice and water clouds from the MFRSR measurements alone, but other sensors can provided information of cloud type enabling proper application of the appropriate fitting results for accurate retrieval of thin cloud optical depths. Even without knowledge of cloud type this technique provides information on the bounds of possible optical depth for thin clouds in general. A source of uncertainty in the retrieval results from the differences between the idealized phase functions used and the phase function of real cloud, particularly cirrus cloud composed of ice crystals with complex shapes. Based on sensitivity analysis, we conclude that the uncertainty associated with real phase function will introduce an additional 5% error into the retrievals with respect to ice or water clouds.

[21] The left panel of Figure 4 shows the simulated and the fitted transmittances from the MFRSR for cirrus clouds with a solar zenith angle of 45 degrees, as well as the direct transmittance without contamination by forward scattering. It exhibits an excellent agreement between the fitted and simulated values, indicating that a good fitting function was selected. The right panel of Figure 4 shows the comparison

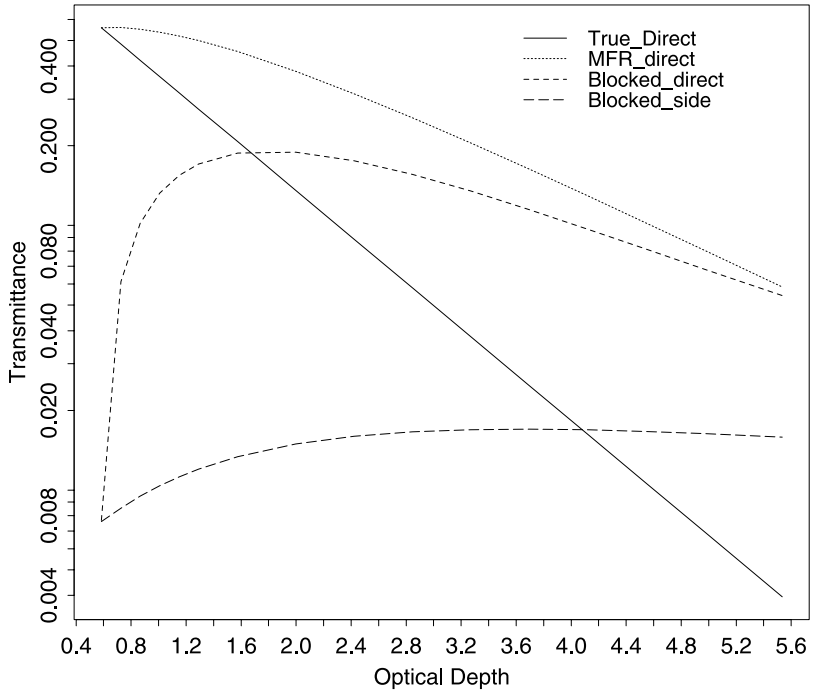

Figure 3. Simulated direct beam measurements of MFRSR as a function of optical depth, and other blocked components.

of the true and inferred optical depths. The apparent optical depth (without correction of forward scattering, "P" in the Figure) is substantially smaller than the true optical depth, and the difference increases with increasing cloud optical depth. The inferred true optical depth (with correction of forward scattering, "C" in the Figure) agrees well with the true optical depth. The difference is less than 5% at the high end of optical depth, and less than 0.01 at the opposite extreme (less than 16% for the true optical depth of 0.05).

4. Observational Results and Validation

[22] The ARM SGP site has been equipped with a suite of instruments to study clouds and radiation transfer. We apply our retrieval algorithm to MFRSR measurements obtained at the ARM SGP site. The MFRSR has been continuously operated at the site for a decade, and more than 60 Langley events have been obtained each year. The solar constants at the passband obtained from Langley regressions are interpolated and extrapolated to any particular day by using a temporal and spectral analysis procedure [*Forgan*, 1988]. The accuracy of solar constant at a non-gaseous absorption passband, based on the Langley regression calibration, is within 1% [*Michalsky et al.*, 2001]. Therefore, we expect the transmittance under cloudy conditions to be better than 1%.

[23] Cloud vertical profiles are observed by a zenith-pointing millimeter-wave cloud radar (MMCR), which is located within about 100 m of the radiation instruments. The upper panel of Figure 5 shows reflectivity from the MMCR that was observed on March 13, 2000 using the algorithm of *Clothiaux et al.* [2000]. The Figure shows the passage of two cirrus clouds over the site separated by a clear-sky gap that extended for 15:30 to 16:20 UTC. The bottom panel of Figure 5 shows cloud and aerosol optical depths inferred from measurements of the MFRSR obtained during the same period. In the Figure, we also indicate the apparent optical depth from which the forward scattering contribution has not been removed. Note that there is a 15-minute shift of the clear-sky gap between the two measurements due to the different viewing geometries of the instruments: a zenith-viewing radar vs. a sun-viewing MFRSR. During the clear-sky gap, the mean aerosol optical depth was 0.12 with the maximum exponent coefficient of 1.2. Therefore, the threshold for discriminating between the cloud and aerosols present is 1 in this case. Aerosol optical depth changes slightly with a mean of 0.22. The cirrus cloud optical depth varies from 0 to 7.2, which is almost twice as much as apparent optical depth. A gap of no data between 20:35 and 20:45 UTC for the apparent optical depth is due to a decrease of the observed direct beam tramsmittance below the minimum detection limit of the MFRSR (0.001).

Table 1. The Quadratic Fitting Coefficients for Both Water and Cirrus Clouds (x.yyy(−z) = x.yyy*10^{-z})

	Cirrus Clouds			Water Clouds		
Fitting Coefficients	SZA < 45	45 ≤ SZA ≤ < 60	SZA > 60	SZA < 45	45 ≤ SZA ≤ < 60	SZA > 60
a	1.0012(−1)	7.3666(−2)	2.1275(−1)	4.4072(−1)	4.5933(−1)	5.0184(−1)
b	9.9163(−2)	1.0157(−1)	4.7279(−2)	5.6432(−2)	3.4323(−2)	1.9060(−2)
c	−6.9077(−3)	−6.6366(−3)	−8.3665(−3)	−3.9574(−3)	−1.4008(−3)	−5.1718(−3)
d	3.1320(−1)	3.2124(−1)	2.6392(−1)	1.8300(−1)	1.8534(−1)	1.7050(−1)

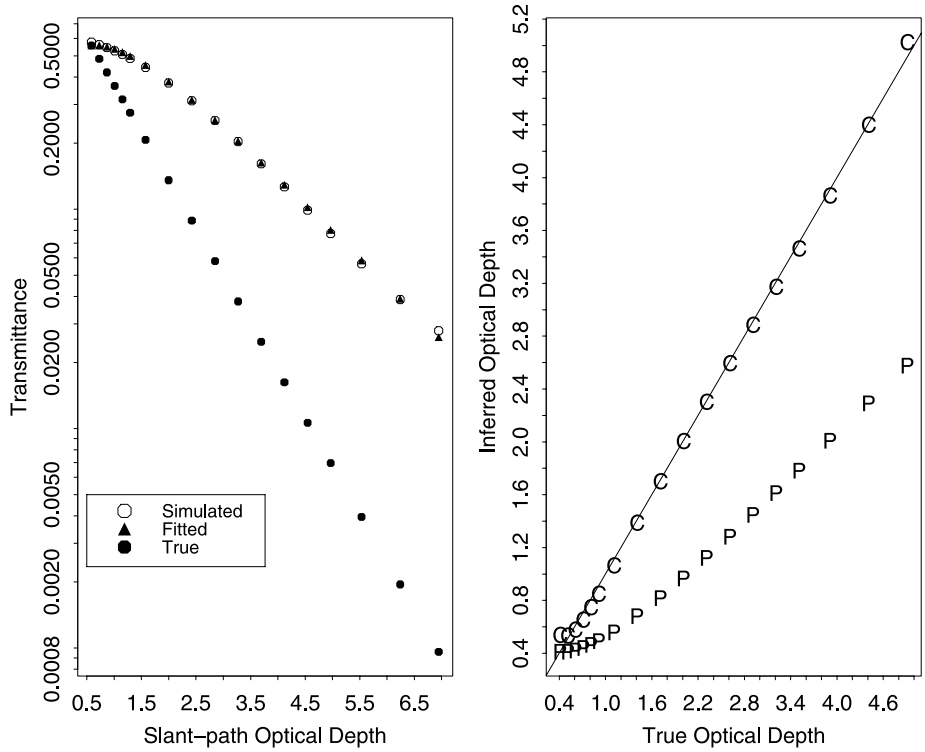

Figure 4. The simulated and fitted transmittances of a MFRSR, and transmittance without forward scattering (solid dot); and the scattergram of true optical depths, inferred apparent optical depths (P), and inferred optical depths with forward scattering correction (C).

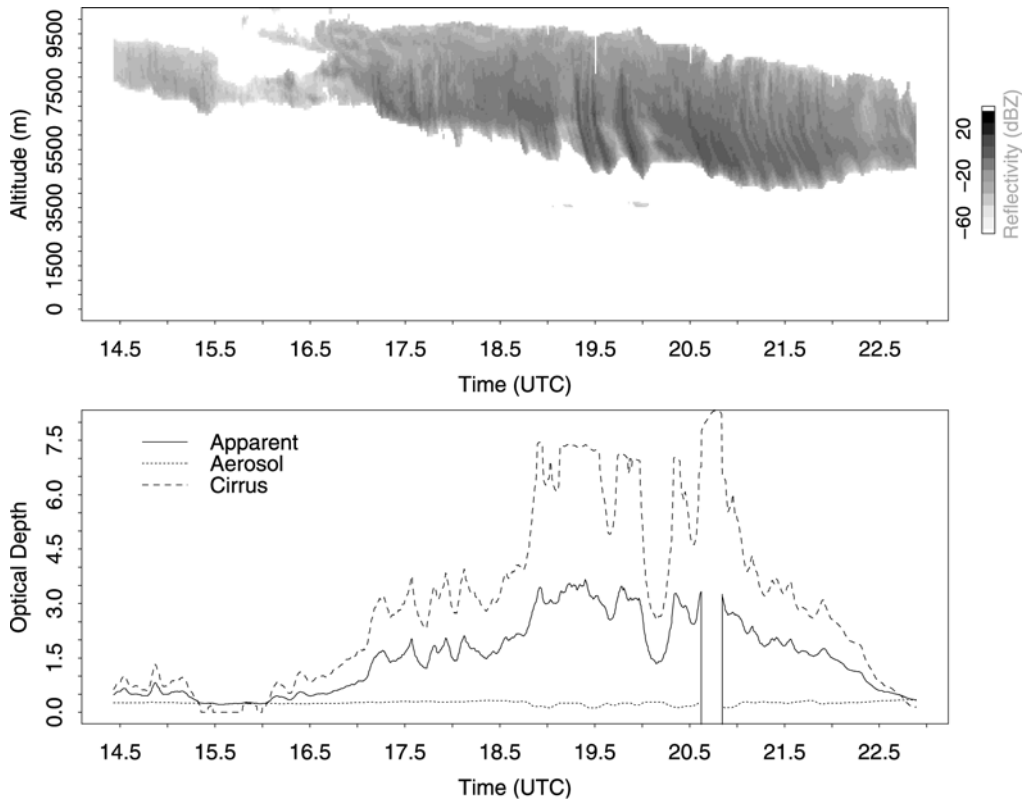

Figure 5. The reflectivity of cirrus cloud measured by the MMCR, and inferred optical depths of aerosol and cloud at the ARM SGP site on March 13, 2000.

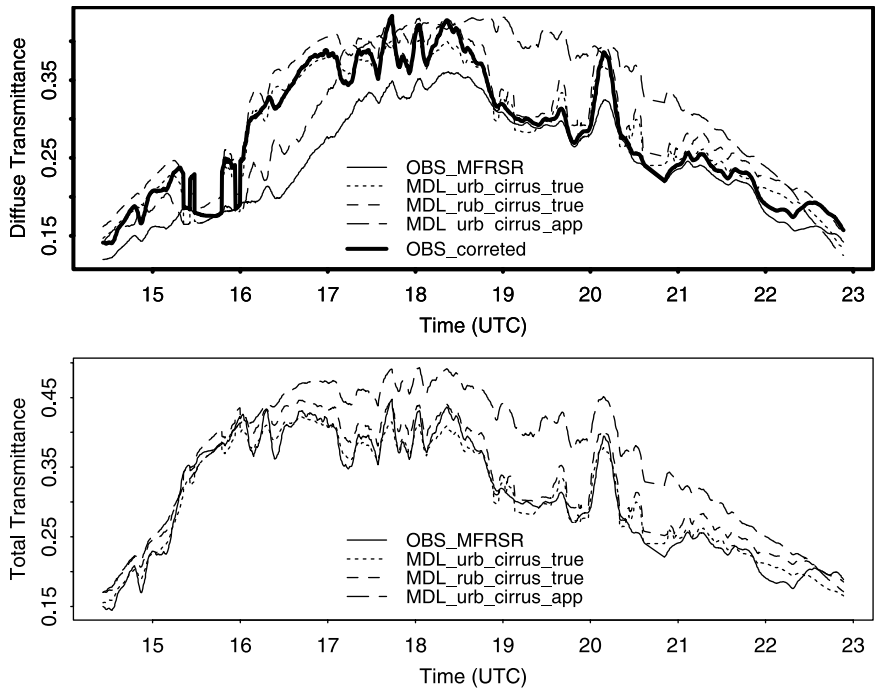

Figure 6. The comparisons of observed and modeled diffuse and total transmittances.

During this period, the cloud optical depth is inferred from diffuse transmittance of the MFRSR at 415 nm using the NLSM algorithm [*Min and Harrison*, 1996a]. It is worthwhile to note that the minimum detection limit of a MFRSR determines the maximum detectable slant optical depth of the cloud. The maximum detectable optical depth for clouds changes with the solar zenith angle.

[24] The MFRSR simultaneously measures the direct normal, diffuse and global irradiances by a blocking technique. As pointed out previously, it guarantees that the measured spectral irradiances are self-consistent and that the accuracy of all components is the same. We take advantage of this to check the consistency of the results for inferred optical depths determined above. We input our inferred optical depths for aerosols and clouds from the direct beam component into a radiation transfer model, and then compare the modeled diffuse and global irradiances with measurements from the MFRSR. In the simulation, we assume the surface albedo to be 0.036. Figure 6 shows the comparison of observed and modeled diffuse and total transmittances. Comparison of transmittances instead of irradiances avoids the uncertainty associated with the extraterrestrial solar spectrum used in the radiative transfer model [*Harrison et al.*, 2003]. To ensure consistency in the comparison, we have to also correct the observed diffuse irradiance to restore the amount of that component that passes through the FOV of the MFRSR and thus, is blocked by the shadow band. The corrected diffuse transmittance can be written as

$$I_{corr}^{dif} = I_{obs}^{dif} + \mu_0\left(\exp\left[-\tau^P/\mu_0\right] - \exp\left[-\tau^T/\mu_0\right]\right) \qquad (11)$$

where τ^T and τ^P are total optical depth in the column of the atmosphere with and without forward scattering correction, respectively. No correction is applied during the clear-sky period, When τ^P (and eventually τ^T) is large under cloudy conditions, the correction will be small as expected. Since there are no direct measurements of the single scattering albedo (SSA) and phase function of aerosols for this case, we use two sets of values to represent these properties in our calculation: 0.96 and 0.92 for the SSA and 0.76 and 0.70 for the asymmetry factor to represent rural and urban aerosols, respectively. The modeled diffuse transmittances with apparent cirrus optical depth does not agree with either the corrected or uncorrected measurements of diffuse transmittances. Alternatively the model diffuse transmittances that are calculated using the true cirrus optical depth agree reasonably well with the corrected diffuse transmittances of the MFRSR; the former lies between the results under rural and urban aerosol conditions, as shown in the top panel of Figure 6. The same conclusion can be drawn from the comparison of total transmittances, shown in the bottom panel of Figure 6. The mean differences between measurements and modeled results are 5% and 6% for rural and urban aerosol condition, respectively. These results validate our retrieval approach and demonstrate that the uncertainty of the inferred results is about 6%.

5. Summary

[25] In this research we develop an accurate retrieval method of thin-cloud optical depth from surface-based measurements of a narrow band radiometer. Thin-clouds occur frequently on a global scale, and thus are climatically important. Additionally, the presence of thin cirrus clouds can affect the accuracy of space-based observations of atmospheric and surface properties. Accurate surface based retrieval of thin cirrus optical depth is valuable for evalu-

ating and enhancing the consistency of space-based measurements that are directed at improving global observations of thin cirrus clouds.

[26] The retrieval method that we develop is based on solar direct beam observations of the MFRSR, which is a seven-channel radiometer with six passbands of 10 nm FWHM centered near 415, 500, 610, 665, 862, and 940 nm, and an unfiltered silicon pyranometer. The instrument has not only been operating at the ARM SGP site for almost a decade, but is currently deployed at numerous sites globally. For the retrieval we take advantage of simultaneous spectral measurements of direct and diffuse transmittance of the MFRSR and temporal and spectral variations in the observed clouds and aerosols. Under conditions of optically thin clouds, particularly clouds with ice crystals, sensors, such as the MFRSR, with a finite FOV observes not only the attenuated direct solar beam but also radiation that has been forward scattered by cloud particles into the instrument's FOV. This introduces a measurement error that is significant at low cloud optical depths. This issue was most recently addressed by *Joseph and Min* [2003]. We develop a simple correction scheme that effectively removes this error. Specifically a polynomial fitting technique is developed from simulated measurements of the MFRSR for a range of atmospheric conditions. The simulations are conducted using a modified DISORT code that can accurately compute radiative intensity for strong forward scattering by thin cirrus and water clouds. Results from analysis of the uncertainty of the method show that it produces retrievals that are better than 5% or 0.05 when cloud optical depth is less than 1.

[27] The retrieval method with the correction technique is validated with observations collected at the ARM SGP site during and intensive observation period. A case study period on March 13 2000 where thin cirrus is present with broken periods is selected from review of Radar data. The retrieval method is applied to obtain the cloud and aerosol optical depths throughout the period. The consistency of the retrieved optical depths are then tested by incorporating them into a radiative transfer model to simulate the total, direct and diffuse transmittances at the surface and comparing the modeled transmittances to observation. Differences between the observed and simulated transmittances suggest that the retrieved optical depths have an uncertainty of about 6%.

[28] **Acknowledgments.** This research was supported by the Office of Science (BER), U.S. Department of Energy, Grants DE-FG02-03ER63531, and Northeast Regional Center of the National Institute for Global Environmental Change (NIGEC) under Cooperative Agreement No. DE-FC03-90ER61010. Data were obtained from the Atmospheric Radiation Measurement (ARM) Program sponsored by the U.S. Department of Energy, Office of Energy Research, Office of Health and Environmental Research, Environmental Sciences Division.

References

Angstrom, A. (1929), On the transmission of sun radiation and on dust in the air, *Geogr. Ann.*, *2*, 156–166.

Baker, H., and A. Marshak (2001), Inferring optical depth of broken clouds above green vegetation using surface solar radiometer measurements, *J. Atmos. Sci.*, *58*, 2989–3006.

Berk, A., L. S. Bernstein, and D. C. Robertson (1989), MODTRAN: A moderate resolution model for LOWTRAN7, *Rep. AFGL-TR-89-0122*, Air Force Geophys. Lab., Hanscom, AFB, Ma.

Clothiaux, E. E., et al. (2000), Objective determination of cloud heights and radar reflectivities using a combination of active remote sensors at the ARM CART sites, *J. Applied Meteo.*, *39*, 645–665.

Dong, X., et al. (1997), Microphysical and radiative properties of boundary layer stratiform clouds deduced from ground-based measurements, *J. Geophys. Res.*, *102*, 23,829–23,843.

Forgan, B. W. (1988), Sun photometer calibration by the ratio-langley method, in *Baseline Atmospheric Program (Australia) 1986*, edited by B. W. Forgan and P. J. Fraser, 22–26, Bur. Of Meteoral., Melbourne, Australia.

Fu, Q. (1996), An accurate parameterization of the solar radiative properties of cirrus, *J. Clim.*, *9*, 2058–2082.

Hansen, J. E., and L. D. Travis (1974), Light scattering in planetary atmospheres, *Space Sci. Rev.*, *16*, 527–610.

Harrison, L. C., and J. J. Michalsky (1994), Objective algorithms for the retrieval of optical depths from ground-based measurements, *Appl. Opt.*, *33*, 5126.

Harrison, L. C., J. J. Michalsky, and J. Berndt (1994), Automated multifilter rotation shadowband radiometer: An instrument for optical depth and radiation measurements, *Appl. Opt.*, *33*, 5188.

Harrison, L. C., M. Beauharnois, J. Berndt, P. Kierdron, J. Michalsky, and Q.-L. Min (1999), The rotating shadowband spectroradiometer (RSS) at the Southern Great Plains (SGP), *Geophys. Res. Lett.*, *26*, 1715–1718.

Harrison, L., P. Kiedron, J. Berndt, and J. Schlemmer (2003), Extraterrestrial solar spectrum 360–1050 nm from Rotating Shadowband Spectroradiometer measurements at the Southern Great Plains (ARM) site, *J. Geophys. Res.*, *108*(D14), 4424, doi:10.1029/2001JD001311.

Hu, Y. X., and K. Stamnes (1993), An accurate parameterization of the radiative properties of water clouds suitable for use in climate models, *J. Clim.*, *6*, 728.

Hu, Y.-X., B. Wielicki, B. Lin, G. Gibson, S.-C. Tsay, K. Stamnes, and T. Wong (2000), δ-Fit: A fast and accurate treatment of particle scattering phase functions with weighted singular-value decomposition least-squares fitting, *J. Quant. Spectrosc. Radiat. Transfer*, *65*, 681–690.

Intergovernmental Panel on Climate Change (IPCC) (2001), *Climate Change 2001: The Third Assessment Report*, edited by J. J. McCarthy, Cambridge Univ. Press, New York.

Joseph, E., and Q. Min (2003), Assessment of multiple scattering and horizontal inhomogeneity in IR radiative transfer calculations of observed thin cirrus clouds, *J. Geophys. Res.*, *108*(D13), 4380, doi:10.1029/2002JD002831.

Junge, C. E. (1963), *Air Chemistry and Radioactiveity*, Academic, San Diego, Calif.

King, M., S. C. Tsay, S. E. Platnick, M. Wang, and K. L. Liou (1997), Cloud retrieval algorithms for MODIS: Optical thickness, effective particle radius, and thermodynamic phase, ATBD-MODIS, NASA, Greenbelt, Md.

Leontieva, E., and K. Stamness (1996), Remote sensing of cloud optical properties from ground-based measurements of transmittance: A feasibility study, *J. Appl. Meteorol.*, *35*, 2011–2022.

Marshak, A., Y. Knyazikhan, A. B. Davis, W. J. Wiscombe, and P. Pilewskie (2000), Cloud-vegetation interaction: Using of normalized difference cloud index for estimation of cloud opical thickness, *Geophys. Res. Lett.*, *27*, 1695–1698.

Matrosov, S. Y., B. W. Orr, R. A. Kropfli, and J. B. Snider (1994), Retrieval of vertical profiles of cirrus cloud microphysical parameters from Doppler radar and infrared radiometer measurements, *J. Appl. Meteorol.*, *33*, 617–626.

Michalsky, J. J., J. A. Schlemmer, W. E. Berkheiser, J. L. Berndt, L. C. Harrison, N. S. Laulainen, N. R. Larson, and J. C. Barnard (2001), Multiyear measurements of aerosol optical depth in the atmospheric radiation measurement and quantitative links programs, *J. Geophys. Res.*, *107*, 12,099–12,107.

Min, Q.-L., and L. C. Harrison (1996a), Cloud properties derived from surface MFRSR measurements and comparison with GOES results at the ARM SGP site, *Geophys. Res. Lett.*, *23*, 1641.

Min, Q.-L., and L. C. Harrison (1996b), An adjoint formulation of the radiative transfer method, *J. Geophys. Res.*, *101*, 1635.

Min, Q.-L., L. C. Harrison, and E. Clothiaux (2001), Joint statistics of photon path length and cloud optical depth: Case studies, *J. Geophys. Res.*, *106*, 7375–7386.

Nakajima, T., and M. Tanaka (1988), Algorithms for radiative intensity calculations in moderately thick atmospheres using a trucation approaximation, *J. Quant. Spectrosc. Radiative Transfer*, *40*, 51–69.

Raschke, R. A., and S. K. Cox (1983), Instrumentation and technique for deducing cloud optical depth, *J. Climate Appl. Meteorol.*, *22*, 1887–1893.

Shiobara, M., and S. Asano (1994), Estimation of cirrus optical thickness from sun photometer measurements, *J. Appl. Meteor.*, *33*, 672–681.

Slingo, A. (1989), A GCM parameterization for the shortwave radiative properties of water clouds, *J. Atoms. Sci.*, *46*, 1419.

Stamnes, K., S.-C. Tsay, W. J. Wiscombe, and K. Jayaweera (1988), Numerical stable algorithm for discrete-ordinate-method radiative transfer in multiple scattering and emitting layered media, *Apllied Optics*, *27*, 2502–2509.

Takano, O., and K.-N. Liou (1989), Solarradiative transfer in cirrus clouds. Part I. Single-scattering and optical properties of hexagonal ice crystals, *J. Atmos. Sci.*, *46*, 3–19.

Wiscombe, J. W. (1977), Delta-M method: Rapid yet accurate radiative flux calculations for strongly asymmetric phase functions, *J. Atmos. Sci.*, *34*, 1408–1422.

M. Duan and Q. Min, Atmospheric Sciences Research Center, State University of New York, Albany, NY 12203, USA.

E. Joseph, Department of Physics and Astronomy, Howard University, Washington, DC 20059, USA.